Journal of the Korean Society of Remote Sensing, Vol. 9, No. 2, 1993

Tropical Plume에 대한 TOVS 추정 가강수량의 평가와 상호비교

정 효 상, 신 동 인
기 상 청, 위성 담당

Evaluation and Intercomparisons of the Estimated TOVS Precipitable Waters for the Tropical Plume

H. S. Chung and D. I. Shin
Korea Meteorological Administration, Satellite Division

요 약

열대 및 아열대 대평양상에서 TOVS(Tiros Operational Vertical Sounder) 가강수량의 추정을 위한 모형을 사용하여 열대 기상 중 하나인 TP(Tropical Plume) 또는 Flare-up 현상의 수증기장을 분석하였다. 전가강수량 모형 (71.1 % 의 변량과 0.62 g cm^{-2}의 표준편차)와 중대류고도 모형(71.7의 변량과 0.17 g cm^{-2}의 표준편차)을 선택하여 Tropical Plume 현상에 대해 TOVS 가강수량, ECMWF(European Centre of Medium Range Weather Forecasts) 가강수량, SMMR(Scanning Multichannel Microwave Radiometer) 가강수량과 OLR(Outgoing Longwave Radiation)을 상호비교하고 평가하였다.

TOVS 가강수량 모형으로는 Tropical Plume이 단지 초기단계인 상층운과 얇은 중층운으로 이루어졌을 때는 이 현상을 식별하기 어려웠으나 발달단계인 상층운과 짙은 중층운이 존재할 때는 이 현상이 뚜렷하였다. ECMWF 가강수량은 종관 기상현상은 잘 설명하였으나 Tropical Plume은 뚜렷하지 않았으며, 열대 수렴대와 남대평양 수렴대에서는 대체로 TOVS 가강수량보다 과습하였다. SMMR 가강수량도 TOVS 가강수량과 비슷한 현상을 보였으나 특히, OLR은 Tropical Plume 현상이 가장 뚜렷이 나타났다.

Journal of the Korean Society of Remote Sensing, Vol. 9, No. 2, 1993

Abstract

Precipitable Waters(PW) are retrieved over the tropical and subtropical Pacific Ocean from TOVS infrared and microwave channel brightness temperature and OLR observations by means of stepwise linear regression. The retrieved TOVS PW fields generated by PW_{sfc}(71.1 % of the variance and 0.62 g cm^{-2} standard error over the surface) and PW_{700500}(71.7 % and 0.17 g cm^{-2} over the 700 - 500 hPa layer) revealed more evolving synoptic signals over the tropical and subtropical Pacific Ocean. The PW_{sfc} does not show significantly the TP feature because of the representation of the lower PW for high-level clouds not associated with deep convection. There exists some elusion to trace the TP on the PW_{sfc} field if any supplementary information does not provide. But ECMWF analysis has a general tendency of drying the subtropics and moistening the ITCZ (InterTropical Convergence Zone) and SPCZ(South Pacific Convergence Zone). However, although ECMWF analysis is fairly successful in capturing mean patterns, it is unsuccessful in following active synoptic signal like a tropical plume.

Similarly, SMMR-PW does not represent the TP well which consists of the high- and middle-level clouds, but PW_{sfc} shows underestimated moistness of TP and does not depict significant signal of TP. In the PW field derived from microwave observations, the TP can not be recognized well. Furthermore, the signature of PW_{sfc} was different from OLR for the TP, which implies the presence of high- and middle-layer thin clouds, but in a closer agreement for deep and active convection areas which contain thick middle- and lower-layer clouds; though OLR represented the cloudiness in the tropics well. In synoptically active regions, it differed from OLR analysis, primarily because of actual differences in water vapor and cloud features. The signature of PW_{sfc} was different from OLR for the TP.

1. Introduction

Meteorological satellite observations can provide much needed information on global and regional moisture distribution at higher temporal resolution. Direct retrieval of important hydrometeorological variables from satellite observations of IR and microwave spectra have not been achieved fully because of the coarse vertical resolution of the inverse methods and inverse problem of the radiative transfer equation for retrieving temperature and moisture profiles(Le Marshall 1988).

PW derived from TOVS observations appears very useful for various studies of the hydrological cycle(Cadet and Greco 1987), as well as for the initialization of numerical weather models(Bengtsson and Shukla 1988). The estimated PW in the atmosphere can be retrieved from linear combinations of the individual satellite channel Brightness Temperature(BT) observations in InfraRed(Aoki and Inoue 1982; Chedin and Scott 1985; Chester et al. 1987; Lipton et al. 1986; McMillin and Crosby 1984; Smith and Woolf 1976; Tjemkes and Stephens 1990) and in micro-wave bands(Alishouse et al. 1990; Staelin et al. 1976; Wang et al. 1989; Wilheit 1990). A better understanding based on more accurate analysis of moisture fields retrieved from satellite observations is needed to improve analysis and prediction of tropical weather features on the spatial and temporal synoptic scale(McGuirk et al. 1985; Smith 1989).

The primary goals of this study are to estimate and to compare the vertical and horizontal distributions of TOVS PW with ECMWF-PW, SMMR-PW, and OLR for a tropical weather feature over the tropical and subtropical regions, especially for a TP(McGuirk et al. 1985) or 'flare-up' phenomenon(Dvorak and Smigielski 1990).

2. Data

2. 1 Data Sources and Types

The primary center for archiving of TOVS data is National Environmental Satellite Data and Information Service(NESDIS) in Washington, D.C., while the SMMR data are archived by the National Space Science Data Center(NSSDC) in Greenbelt, Maryland. Descriptions of the observing systems and summaries of satellite data collected can be found in the NOAA Polar Orbiter Data User's Guide, in Smith et al.(1979) for TOVS and in the User's Guide for the Nimbus-7 SMMR CELL-ALL Tape. Corrections applied to the CELL data are presented by Gloersen(1987) for radiometric calibration, polarization mixing, sun shining in the cold horn and beam spill-over into space. OLR at the top of the atmosphere is a strong function of the cloud top temperature, and when averaged over large tropical areas, provides a good index for the areal coverage of deep convective activity. The ECMWF and OLR data used in this study are archived by National Center for Atmospheric Research(NCAR).

2. 2 Various Precipitable Water Fields

For data collection processes, these observations are considered coincident with TOVS observations when they are within 5 h, and within 0.5° or 1.0° in latitude and longitude of the TOVS observations. The region examined in this study extends from 150°E to 100°W longitude, and from 30°S to 30°N latitude for January 1983. In this study 1.0 g cm^{-2} PW is equivalent to 10.0 kg m^{-2} PW or 10.0 mm PW. Seven available data sets are generated from January 11 to 23, 1983; with 2.5° grid. Due to the large gaps between the swaths of SMMR observations, SMMR-PW field is mapped by contouring over the limited area where the data are available. Eymard et al.(1989) pointed out that SMMR data has an abnormal high temperature found in the northern part of the tropical Pacific Ocean due to the SMMR attitude drifting during each orbit, causing incidence angle variations reaching 1.5° to 2° near the poles. This results in greater surface emissivity, longer path length of the earth rotation, and error on the surface pixel location.

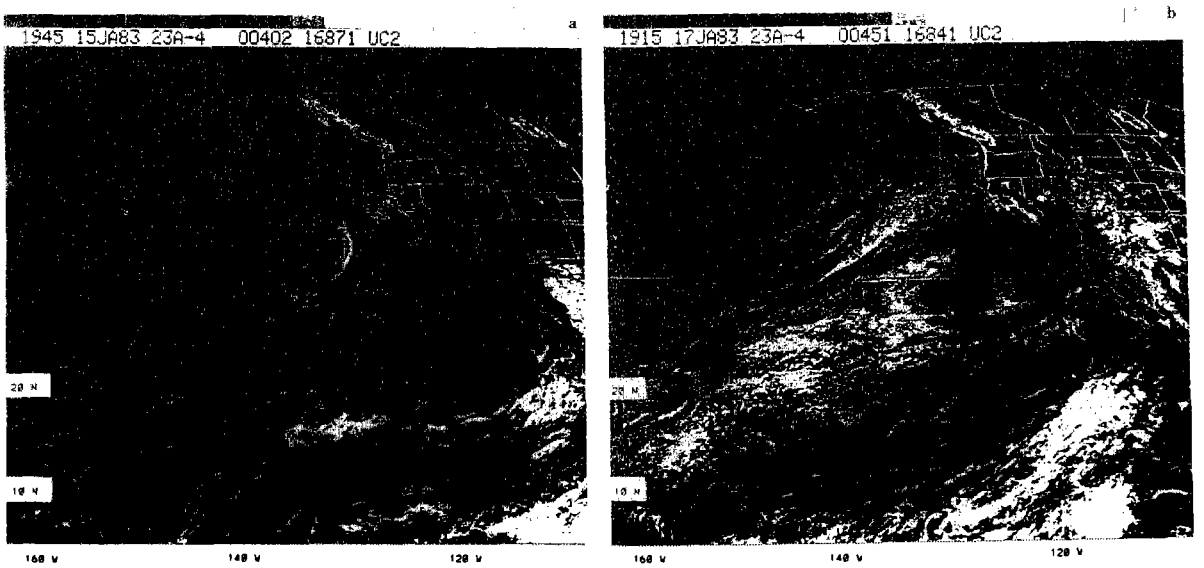

Fig. 1. a) Enhanced window GOES WEST satellite photograph for January 15, 1983 for the tropical quiescent case and b) for January 17, 1983 for the tropical plume case originated at 8° N and 130° W.

The absolute magnitude, maximum and minimum and matchup of synoptic features of TOVS PW fields are investigated and compared with other data fields. For January 15, 1983 during the time periods of interest, a relatively quiescent synoptic case is shown in Fig. 1a; by January 17, 1983 a tropical system, called a TP, has developed as shown in Fig. 1b described by Smith(1989). Figure 1a is a section of the GOES IR window channel imagery, at 1945 UTC 15 January 1983 for the quiescent case. Figure 1b shows the leading edge of the TP at 1915 UTC January 17, 1983 which reached 20° N and 115° W. In Fig. 1, the synoptic features of the tropical atmosphere can be detected easily. The TP is originated from 8° N and 130° W in Fig. 1b. For both cases PW fields derived from TOVS BTs, ECMWF analysis, SMMR BTs and OLR are mapped and compared.

The TP defined by McGuirk et al.(1987) is largely geometric and based on unenhanced window channel IR imagery, but is called as Flare-up defined by Dvorak and Smigielski(1990), which is most prevalent during winter season over the tropical eastern Pacific and eastern Atlantic Oceans of the Northern Hemisphere. A typical TP in IR imagery might represent a cloud band of at least synoptic scale, 2000 km or greater. Currently there is a lack of ground-truth measurements in the domain and time periods of interest. None of these data sources depict the atmospheric moisture structure sufficiently well to evaluate its retrieval satisfactorily.

3. Retrieval of TOVS PWs

3. 1 Retrieval of PW_{sfc}

The fitted model for retrieving PW_{sfc} from RAOB requires 14 independent variables which explained 71.1 % of the variance with a rms error of 0.622 g cm^{-2} as listed in Table 1(refer to Chung 1993). The most important independent variables for explaining variations in the data were BTs of the lowest thermal and water vapor sensitive channels 14, 7, 6 and 10 rather than those of water vapor channels 11 and 12. These are not surface, but near surface (1000 - 800 mb), temperature sensitive channels. In particular Channel 14 is in the 4 μm band, supposedly, less sensitive to water vapor than channel 7 in the 14 μm band. Water vapor channel 10 explains only 10 % of total variance in the model and is mostly thought of as a temperature channel in the troposphere. These regression

Table 1. Statistical properties of the fitted model to retrieve PW_{sfc}.

Variable name(°C)	Partial of R^2	Parameter constant(B_i)	Standard error	t-probability
Intercept(B_0)	0.0000	-14.71045	46.07134	0.7496
HIRS14	0.3209	9.14741	0.82385	0.0001
HIRS7	0.2504	-2.37499	0.35962	0.0001
HIRS10	0.0526	-0.67395	0.47133	0.1531
HIRS6	0.0227	-3.11398	0.80478	0.0001
QSTAB4	0.0178	26.33130	3.88793	0.0001
HIRS13	0.0130	-2.98835	0.48203	0.0001
HIRS3	0.0094	-1.12401	0.19969	0.0001
HIRS21	0.0058	0.51807	0.07291	0.0001
HIRS19	0.0053	-1.57613	0.58715	0.0074
HIRS18	0.0051	2.19537	0.48958	0.0001
QSTAB7	0.0043	-1.76954	0.85751	0.0393
QSTAB3	0.0018	16.31446	7.09768	0.0217
QSTAB5	0.0013	38.35856	36.47634	0.2932
HIRS12	0.0011	0.11485	0.10385	0.2690

Table 2. Statistical properties of the fitted model to retrieve PW_{700500}.

Variable name(°C)	Partial of R^2	Parameter constant(B_i)	Standard error	t-probability
Intercept(B_0)	0.0000	-143.58592	32.06248	0.0001
QSTAB12	0.4383	0.67023	0.10439	0.0001
QSTAB11	0.1537	1.23962	0.17661	0.0001
HIRS12	0.0482	0.07871	0.09327	0.3989
HIRS3	0.0206	-0.40777	0.06833	0.0001
HIRS19	0.0087	-2.62956	0.42011	0.0001
HIRS18	0.0085	1.05012	0.12696	0.0001
QSTAB3	0.0083	-16.79314	3.70884	0.0001
HIRS13	0.0074	-0.69435	0.12332	0.0001
QSTAB6	0.0065	-0.21666	0.15513	0.1628
QSTAB9	0.0057	-5.41532	1.18659	0.0001
QSTAB8	0.0049	0.15886	0.08099	0.0501
HIRS14	0.0030	7.73050	1.55784	0.0001
QSTAB2	0.0022	0.88972	1.25724	0.4793
QSTAB5	0.0015	158.26147	31.11155	0.0001

coefficients and R2 values give a general idea of the individual importance of the variables to TOVS PW. HIRS21(at 0.6 %), QSTAB3 (0.2 %) and HIRS12(0.1 %) are the only truly moisture sensing variables which explain in all but statistically significant variance.

3. 2 Retrieval of PW_{700500}

Table 2(refer to Chung 1993) showed that the fitted regression model for predicting PW_{700500} requires 14 independent variables to explain 71.7 % of the variance in the data yielding yielding a rms error of 0.172 g cm^{-2}. The first three predictors involve moisture channels 10(QSTAB11), 11(QSTAB12) and HIRS12, total 64 % of the variance explained. These were different from major variables of PW_{sfc} estimation. Three variables related to water vapor channels 10, 11 and 12 can explain 89 % of total variation in the model to estimate PW_{700500}. The only other variable explaining more than 1.0 % is HIRS3(2.0 %), a 100 mb temperature channel in the 14 μm band.

As listed in Table 1 and Table 2, the best models chosen were for PW_{sfc} and PW_{700500}. The explained variances, rms errors and the degrees of freedom for the two models, PW_{sfc} and PW_{700500}, were acceptable for this study using real IR and microwave satellite observations alone to retrieve PW by statistical means. This was also due to the fact that PW_{sfc} and PW_{700500} can be determined reasonably well from TOVS observations. Since this procedure is simple to use and provides accurate results, it can be an alternate but useful tool to retrieve atmospheric amoisture terms in the tropics. Furthermore, as long as accurate and useful QSTABs are developed from TOVS observations, the fitted model has low degrees of freedom and achieves higher multiple correlations that better represent tropical weather systems.

4. Evaluation and Intercomparisons of TOVS PWs

There does not exist any actual ground truth to establish the quality of any measurements within the domain of interest except for a few RAOBs. In the absence of a sufficiently dense and reliable network of in-situ measurements on the one hand, and of a higher spatial resolution of microwave observations on the other hand, validation of the retrieved PW field from TOVS observations previously described above is difficult. Intercomparisons of retrieved TOVS PW with ground truth measurements of PW or other

retrieved PW over the oceans are essential to depict systematic errors related to tropical weather systems or to validate interpretation of synoptic scale features in the tropics.

Instead of direct evaluation of the retrieval algorithm of TOVS PW, useful intercomparisons of the predicted TOVS PW fields with other simultaneous satellite-derived PW fields(SMMR-PW and OLR) or numerical analysis field (ECMWF-PW) are carried out. The purpose of this study is to present the results of comparisons of PW_{sfc} and PW_{700500} with ECMWF-PW, SMMR-PW and OLR in the tropics, with regression estimates from TOVS observations. TOVS retrievals are available only in cloud free of cloud cleared regions. Cloudy regions are estimated from spatial interpolation. The other estimates are available in cloudy regions only the horizontal fields of PW_{sfc} and PW_{700500} are evaluated and compared. These not only yield higher multiple correlations (R^2 = 0.711 and 0.717) but also yield relatively lower rms errors and smaller degrees of freedom in the regressions.

4. 1 Retrieved PW Field from TOVS Observations

Evaluation of the PW_{sfc} and PW_{700500} from TOVS observations using the fitted models is carried out for January 15 and 17, 1983. The simultaneous comparison of TOVS PW with SMMR-PW, ECMWF-PW, or OLR is available for the time periods of interest for January 11, 13, 15, 17, 19, 21 and 23, 1983 avoiding the SMMR drifting problem and is achieved. The input variables and coefficients of the fitted regression models from Table 1 and Table 2 make use of generating PW_{sfc} and PW_{700500} with 2.5° horizontal resolution. The independent variables and regression coefficients from these tables put into equation(1), individually and predict PW_{sfc} and PW_{700500}, respectively. In order to have a regular grid in space and time of PW from predicted TOVS PWs an objective analysis was performed by use of the Barnes technique(Barnes 1973). If the consecutive missing grid value with the number 999.9, where there is missing orbit or overcast, is present, then this analysis will take an average of three or four surrounding values again and fill it.

Figure 2 and Fig. 3 represent the contour maps of retrieved a) PW_{sfc} and b) PW_{700500} from TOVS observations for January 15, 1983 for the quiescent case and for January 17, 1983 for the TP case. The contours are labeled every 4 kg m^{-2}. The evolution of TOVS PWs on two layers(PW_{sfc} and PW_{700500}) show the synoptic characters prevailing during the sampling period. The most striking features in both cases are the significant PW_{sfc} of the ITCZ along 5° S except in the extreme eastern Pacific Ocean. This axis matches the cloud

patterns in Fig. 1. Although the SPCZ is not well defined moist extreme extend into the east of Southern Hemisphere, at 15° W on the 15th and east of 13° W on the 17th. The lower PWs to the north are associated with the persistent subtropical subsidence regions.

In the TP case on January 17, 1983, the patterns of lower PW_{sfc}s over the south Pacific subsidence regions are extended to the north at 115° W as shown in Fig. 3a. The eastern edge of the ITCZ is strengthened in the South Hemisphere and becomes better organized in the North Hemisphere as the TP develops out of the ITCZ at 135° W. There is strong evidence of an equatorial wave in the moisture field, 3000-3500 km in wave length, particularly on the 17th. The PW_{sfc} field seems to be slightly different than the PW_{700500} field in the western portion of the ITCZ but similar to the central and eastern side of the

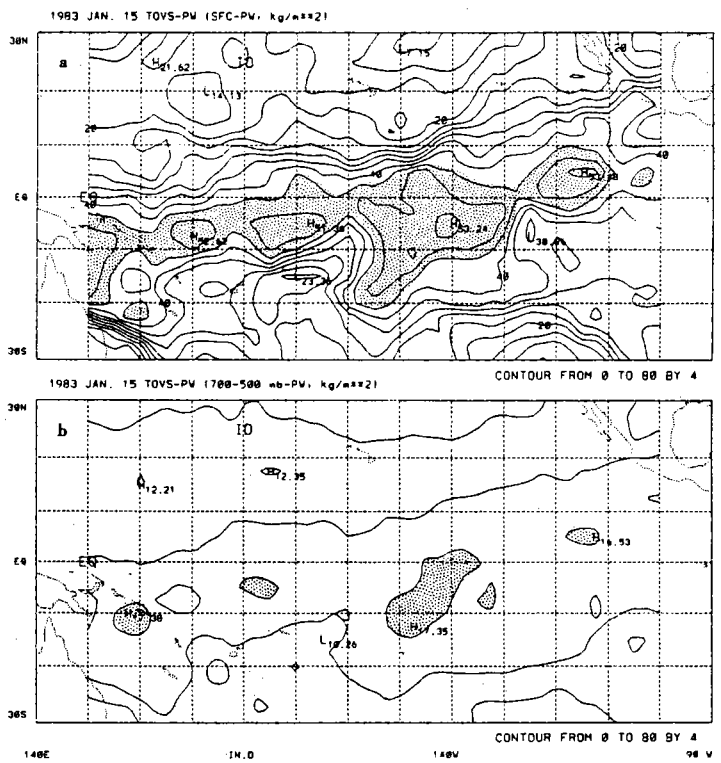

Fig. 2. The mean maps of a) PW_{sfc}(the shaded area represents to be equal to or greater than 44 kg m^{-2}) and b) PW_{700500} predicted by the fitted models for the tropical quiescent case (the shaded area represents to be equal to or greater than 16 kg m^{-2}). The contour interval is 4 kg m^{-2}.

ITCZ. There exists a significant extension of higher PW in the southeastern Pacific Ocean corresponding to the northeastern movement of the TP as shown in Fig. 3a. Drying is observed in the equatorial region to the northwestern side of its plume in Fig. 3.

However, there is marked a little disagreement between TOVS PW and IR imagery for the TP feature. The PW_{sfc} does not show significantly the TP feature because of the representation of the lower PW for high-level clouds not associated with deep convection. If the TP is not associated with the lower- and middle-level thick clouds or precipitation process, PW_{sfc} would be difficult to depict the TP. It is true that there exists some elusion to trace the TP on the PW_{sfc} field if any supplementary information does not provide. The presence of high- or medium-level thin clouds leads to complication of the interpretation of synoptic scale features based on only the PW_{sfc} field.

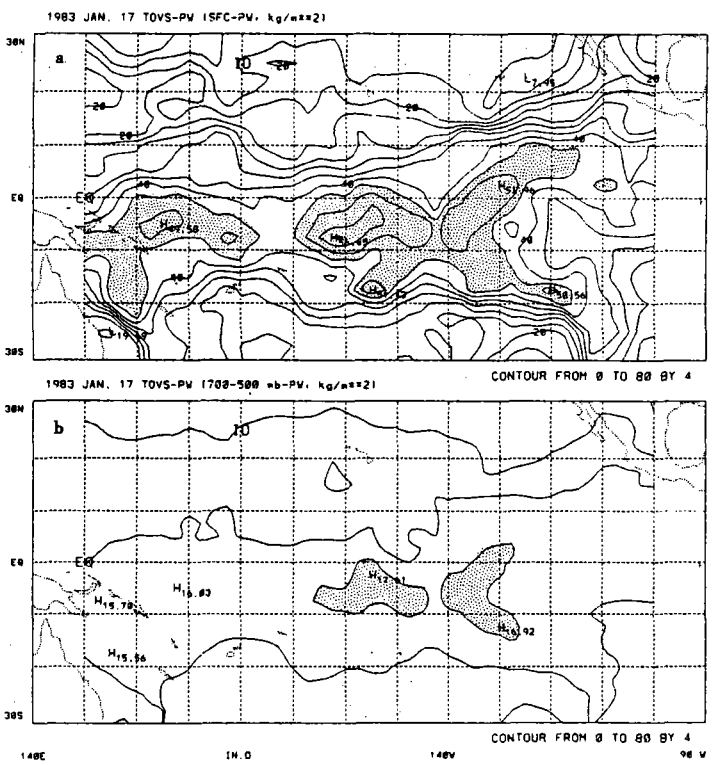

Fig. 3. The mean maps of a) PW_{sfc}(the shaded area represents to be equal to or greater than 44 kg m^{-2}) and b) PW_{700500} predicted by the fitted models for the tropical plume case(the shaded area represents to be equal to or greater than 16 kg m^{-2}). The contour interval is 4 kg m^{-2}.

4. 2 Comparison of TOVS PW and ECMWF-PW

The ECMWF-PW analysis(expressed in kg m^{-2}) is presented in Fig. 4a for the quiescent case and Fig. 4b for the TP case. The contours are labeled every 4 kg m^{-2}. The corresponding maps resulting from TOVS observations are displayed in Fig. 2a and Fig. 3a. One obvious problem with the ECMWF analysis is that it does not resolve any TP features. The quiescent case is drier to the northwestern portion of the TP(Fig. 4a) than is the TP (Fig. 4b). PW_{sfc} indicates drying with the TP. There is no evidence of extension or moistening of the TP axis as it appears in Fig. 3a.

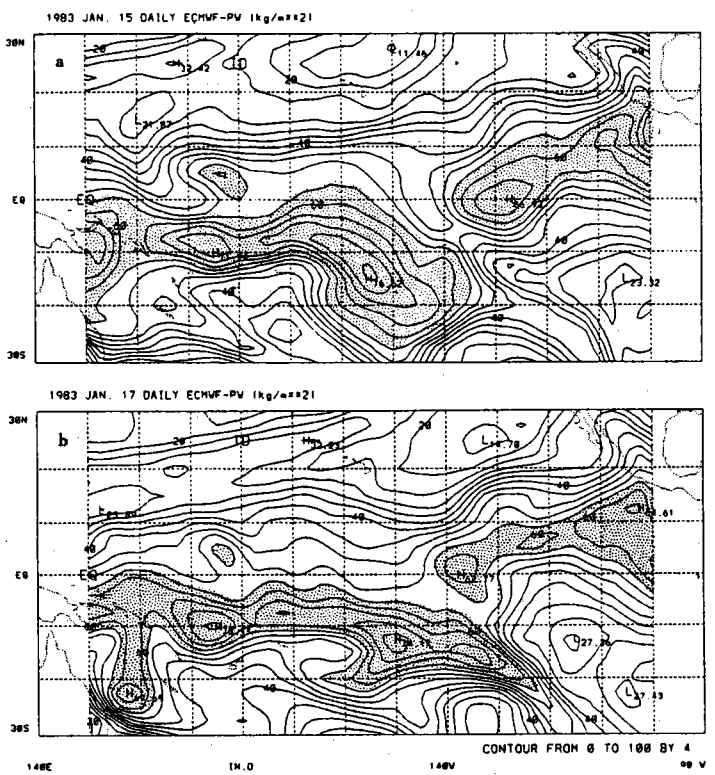

Fig. 4 The maps of ECMWF-PW calculated for a) the tropical quiescent case and b) the tropical plume case. The contour interval is 4 kg m^{-2} and the shaded area represents to be equal to or greater than 56 kg m^{-2}.

Qualitative and quantitative comparisons of the magnitude and coherent pattern of PW_{sfc} with ECMWF-PW are implemented. The ECMWF-PW gradients observed on Fig. 4 are stronger than the ones appearing over the same area on Fig. 2a and Fig. 3a. The wettest areas just below the equator are located approximately at 10° S as shown in Fig. 4 rather than those located at 5° S as shown in Fig. 2a and Fig. 3a. A difference between the TP area identified by VAS imagery as shown in Fig. 1b and by the analysis on Fig. 4b is observed. The pattern of significant wet PW_{sfc} in the ITCZ is elongated to the north-eastern equatorial Pacific Ocean as shown in Fig. 2a, which is similar to that of ECMWF-PW as shown in Fig. 4a for the quiescent case. The largest differences between two horizontal distributions are found in the western ITCZ, the central equatorial Pacific Ocean and dry region of the South Pacific Ocean as shown in Fig. 4.

For the TP case the pattern of wet PW from PW_{sfc} and ECMWF-PW distributions, as shown in Fig. 3a and Fig. 4b, is shifted a little to the north-eastern Pacific Ocean and that of dry PW is expanded to the north-western Pacific Ocean. Here ECMWF-PWs for both cases contain approximately 2.0 g cm^{-2} more than PW_{sfc}s over the ITCZ and the dry regions of the subtropical oceans. Qualitatively, a good relationship between PW_{sfc} and ECMWF-PW is observed; however, the higher resolution of TOVS retrievals result in more detailed information in areas where they are available. However, although ECMWF analysis is fairly successful in capturing mean patterns, it is unsuccessful in following active synoptic evolution.

Heckley(1985) found that ECMWF analysis of the moisture field is too wet in the lower troposphere and that subsidence inversions cannot be maintained realistically. This is partly due to the spinup of the model hydrological cycle which may bias the first guess primarily based on the lack of data. However, the average of ECMWF-PW is overestimated more than PW_{sfc}. In the active ITCZ, SPCZ, western dry region of the North Pacific Ocean and eastern and equatorial dry region of South Pacific Ocean, ECMWF-PW is lower than PW_{sfc} as pointed out by Klinker(1990), but in the eastern dry region of North Pacific Ocean and TP region, ECMWF-PW is higher than PW_{sfc}.

Results of the statistical analysis of TOVS PW against ECMWF-PW from seven data sets show rms values are on the order of 24 % to 32 % of the mean PW, which shows a rough agreement, in the wetter case. RMS error of ECMWF-PW for PW_{sfc} is approximately 0.83 g cm^{-2} and a 0.81 correlation coefficient for 7,106 selected gridded data in the time period of interest(January 11, 13, 15, 17, 19, 21 and 23, 1983).

4. 3 Comparison of TOVS PW and SMMR-PW

SMMR-PW field(expressed in kg m^{-2}) is presented on Fig. 5a for the quiescent case and Fig. 5b for the TP case. The contours are labeled every 4 kg m^{-2}. The corresponding maps resulting from TOVS observations are displayed on Fig. 2a and Fig. 3a. The higher resolution and the interpolation scheme of TOVS retrievals results in more smoothed information on areas where TOVS observations are available. PW_{sfc}s over the west side of ITCZ, SPCZ, western dry regions of North Pacific Ocean, and the eastern dry regions of South Pacific Ocean are about 0.5 g cm^{-2} less than SMMR-PWs for both cases. Especially, PW_{sfc} is drier than SMMR-PW over the eastern dry region of South Pacific Ocean for the TP case. The gradients observed in Fig. 5 are roughly stronger than the ones appearing over the same area for PW_{sfc}. It is obvious that SMMR-PW does not represent the TP well which consists of the high- and middle-level clouds, but PW_{sfc} shows underestimated moistness of TP and does not depict significant signal of TP. In the PW field derived from microwave observations, the TP can not be recognized well.

Chang et al.(1984) found that SMMR-PW climatology is substantially higher over the North Hemisphere than climatologies derived using conventional data, but are in closer agreement over the Southern Hemisphere. Husson et al.(1992) showed that TOVS water vapor content obtained by an Improved Initialization Inversion technique has a mean bias of 0.5 g cm^{-2} for RAOB observations. Tjemkes and Stephens(1990) showed that in the regions of subsidence associated with the air motion around the subtropical zone of high pressure, TOVS observations tend to overestimate PW more than SSM/I-PW. This was due to erroneous interpretation of the attenuation of radiation emerging from the surface by the stratocumulus clouds found in these regions.

However, contoured maps of both PW fields present similar large scale features with mean gradients, magnitudes and patterns. Mean difference between the two fields shows about 0.6 g cm^{-2} in excess for SMMR-PW and some strong local differences, reaching approximately 1.0 g cm^{-2}. Reanalysis of PW_{sfc} and SMMR-PW from the seven data sets resulted in rms differences that are less than 27 % of the mean PW, showing a closest agreement, in the wetter case. RMS error of TOVS PW against SMMR-PW is approximately 0.397 g cm^{-2} with a 0.92 correlation coefficient for 35 selected point-paired observations within the time period of interest(January 11, 13, 15, 17, 19, 21 and 23, 1983).

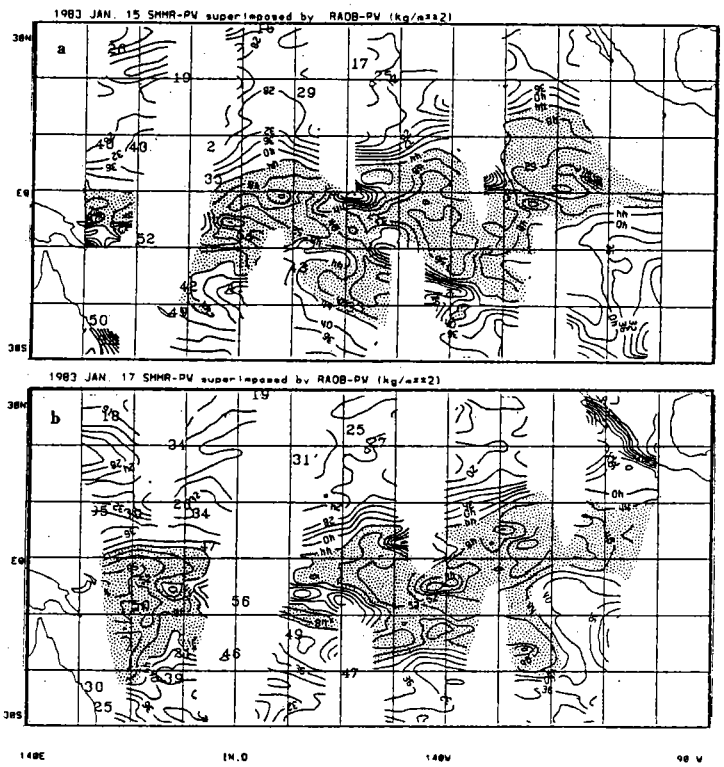

Fig. 5 The maps of SMMR-PW calculated for a) the tropical quiescent case and b) the tropical plume case. The larger font numbers represent RAOB-PWs (kg m^{-2}). The contour interval is 4 kg m^{-2} and the shaded area represents to be equal to or greater than 44 kg m^{-2}.

4. 4 Comparison of TOVS PW and OLR

Direct comparison between TOVS PW and OLR is not possible due to physically different radiative characteristics and observational units. OLR at the top of the atmosphere is widely used to identify the intensity and area coverage of deep convection and the TP in the tropics. High values of OLR are found over large parts of the subtropical oceans indicating a general lack of cloud cover. In the tropics where thermal variations are modest, variations in OLR are dominated by convective cloud tops. The collected data was generated by excluding the extremely dry cases for January 15, 1983 for the quiescent case and for January 17, 1983 for the TP case. Mean maps of OLR depict similar large scale features and cloudiness.

OLR fields(expressed in W m^{-2}/10.) is presented in Fig. 6a for the quiescent case and Fig. 6b for the TP case. The contours are labeled every 4 W m^{-2} after dividing 10. The corresponding maps from TOVS observations are in Fig. 2a and Fig. 3a and show similar

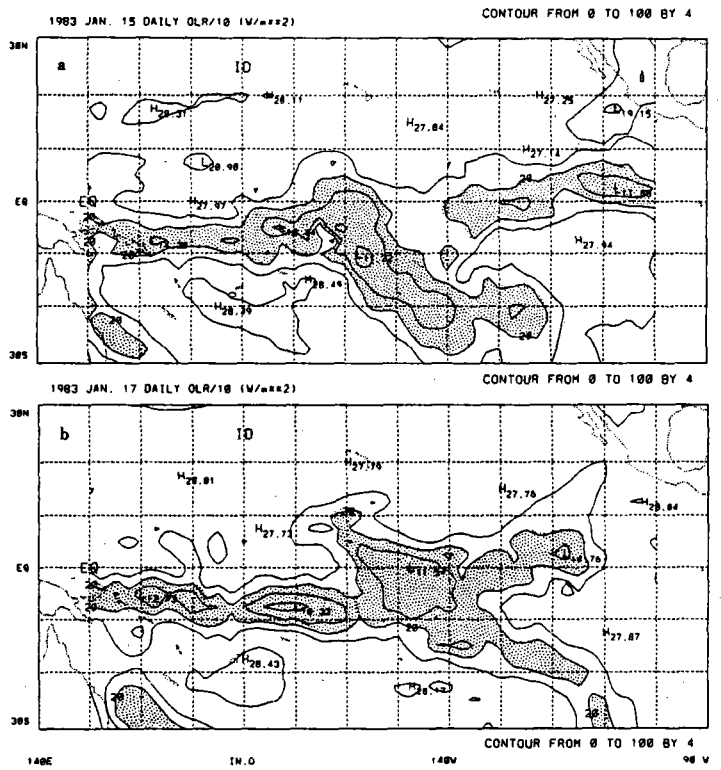

Fig. 6 The maps of OLR for a) the tropical quiescent case and b) the tropical plume case. The shaded area represents to be equal to or less than 200 W m^{-2}/10.0 and the contour interval is 4 W m^{-2}.

wet regions and cloudiness. Figure 6b represents well the TP feature corresponding to Fig. 1b. Qualitative comparisons of their magnitudes, locations of maximum and minimum and patterns between OLR and PW_{sfc} are similar. Qualitatively, maps of OLR represent well the cloudiness or precipitation process observed; however, the OLR field results in more detail in moist or precipitating regions, but the PW_{sfc} field provides more detailed information for the relatively dry regions; on the other hand, TOVS observations predict poorly when OLR is greater than 275 W m^{-2}. The lower value of OLR expands in the north-eastern Pacific Ocean.

Although OLR represents the high- or middle-layer clouds for the TP, the horizontal surface distribution of PW retrieved from TOVS observations is not affected substantially by the upper tropospheric water vapor. Saito and Baba (1988) found that the relation of cloud amount to relative humidity through examination of Geostationary Meteorological Satellite observations is somewhat loose, but it can be considered that the average value of a classified cloud amount is expressed by a quadratic function of the relative humidity.

5. Summary

The chosen fitted models were in a reasonably close agreement to estimates of PW_{sfc} as shown by other studies(Fink and McGuirk 1989; Le Marshall 1988; Reuter et al. 1988). Through error analyses the results calculated from TOVS observations were chosen by two acceptable algorithms resulted for predicting PW_{sfc} and PW_{700500} from TOVS data only. The algorithm of PWsfc explained approximately 71.1 % of the observed variance in the data while rms error was the relatively small(0.622 g cm^{-2}) and the degrees of freedom were minimal with 14 independent variables among the regression equations. The algorithm of PW_{700500} also showed approximately 71.7 % of explained variance in the data while rms error was the also relatively small(0.172 g cm^{-2}) and the degrees of freedom were minimal with 14 independent variables among four vertical regression equations.

The PW_{sfc} does not show significantly the TP feature because of the representation of the lower PW for high-level clouds not associated with deep convection. If the TP is not associated with the lower- and middle-level thick clouds or precipitation process, PW_{sfc} would be difficult to depict the TP. It is true that there exists some elusion to trace the TP on the PWsfc field if any supplementary information does not provide. However, the presence of high- or medium-level thin clouds leads to complication of the interpretation of synoptic scale features based on only the PW_{sfc} field. But ECMWF analysis has a general tendency of drying the subtropics and moistening the ITCZ and SPCZ. However, although ECMWF analysis is fairly successful in capturing mean patterns, it is unsuccessful in following active synoptic evolution.

It was obvious that SMMR-PW does not represent the TP well which consists of the high- and middle-level clouds, but PW_{sfc} shows underestimated moistness of TP and does not depict significant signal of TP. In the PW field derived from microwave observations, the TP can not be recognized well. The signature of PW_{sfc} was different from OLR for the TP, which implies the presence of high- and middle-layer thin clouds, but in a closer

agreement for deep and active convection areas which contain thick middle- and lower-layer clouds; though OLR represented the cloudiness in the tropics well. The presence of high- or medium-level thin cloud led to complication of the interpretation of synoptic scale features based on the PW amount.

In data sparse regions, retrieved TOVS PW can yield a significant contribution to the three dimensional analysis of the atmospheric PW. These algorithms of estimating PW from TOVS observations are simple and useful to interpret and understand the synoptic scale features and to reproduce the climatological PW field in the tropics. For different geographical distributions and the other time periods this procedure should be tested further.

Acknowledgments

This research for developing alternative models for estimating total precipitable water from TOVS observations has been performed under the NASA Global Scale Atmospheric Precesses Research Program. Thanks are especially to Dr. J. McGuirk in Texas A&M University and to several satellite data and information services in the United States preparing moisture analyses.

References

Alishouse, J. C., S. A. Snyder, J. Vongsathorn and R. R. Ferraro, 1990, "Determination of oceanic total precipitable water from the SSM/I.", *IEEE Trans. Geosci. Remote Sensing*, 88 : 811-816.

Aoki, T., and T. Inoue, 1982, "Estimation of the precipitable water from the IR channel of the Geostationary Satellite", *Remote Sensing of Environment*, 12 : 219-228.

Barnes S. L., 1973, "Mesoscale objective map analysis using weighted time-series observations. NOAA Tech.", Memo. ERL NSSL-62 NOAA Washington, D.C., 60pp.

Cadet, D. L., and S. Greco, 1987, "Water vapor transport over the Indian Oceans during the 1979 summer monsoon. Part I; Water vapor fluxes", *Mon. Wea. Rev.*, 115 : 653-663.

Chang, H. D., P. H. Hwang, T. T. Wilheit, T. C. Chang, D. H. Staelin and P. W. Rosenkranz, 1984, "Monthly distributions of precipitable water from the Nimbus 7 SMMR data", *J. Geophys. Res.*, 89 : 5328-5334.

Chedin, A., and N. A. Scott, 1985, "Initialization of the radiative transfer equation inversion problem from a pattern recognition type approach: Applications to the satellites of the TIROS-N series", *Advances in Remote Sensing Retrievals.* Academic Press, Hampton, VA., 495-515.

Chesters, D. L., W. D. Robinson and L. W. Uccellini, 1987, "Optimized retrievals of precipitable water from the VAS split window", *J. Climate Appl. Meteor.*, 26 : 1059-1066.

Chung, H. S. 1993, "Atmospheric moisture fields derived by satellite observations over the tropical Pacific Ocean", Ph. D. Dissertation, Dept. of Meteorology, Texas A&M University, College Station, TX 77843, 167pp.

Dvorak, V. F., and F. J. Smigielski, 1990, *A workbook on tropical clouds and cloud systems observed in satellite imagery.* vol. II.

Eymard, L., C. Klapisz and R. Bernard, 1989, "Comparison between Nimbus-7 SMMR and ECMWF model analyses: The problem of the surface latent heat flux", *J. Atmos. Oceanic. Technol.*, 6 : 866-881.

Fink, J. D., and J. P. McGuirk, 1989, "Tropical synoptic scale moisture fields observed from the Nimbus-7 SMMR.", *Fourth Conf on Satellite Meteorology and Oceanography.* San Diego, CA., Amer. Meteor. Soc., 79-80.

Gloersen, P., 1987, "In orbit calibration adjustment of the Nimbus-7 SMMR.", NASA Rep. 100678, NASA Goddard, Greenbelt, MD., 39pp.

Grody, N. C., A. Gruber and W. C. Chen, 1980, "Atmospheric water content and the tropical Pacific derived from the Nimbus-6 Scanning Microwave Spectrometer", *J. Appl. Meteor.*, 19 : 986-996.

Heckley, W. A., 1985, Systematic errors of the ECMWF operational forecasting model in tropical regions. *Quart. J. Roy. Meteor. Soc.*, 111 : 709-738.

Husson, N., Y. Tahani, C. Cloud, N. A. Scott and A. Chedin, 1992, "NOAA(TOVS) and DMSP(SSM/I) satellite observations for global atmospheric water vapor", *Sixth Conf on Satellite Meteorology and Oceanography.* Atlanta, GA., Amer. Meteor. Soc., 297-300.

Klinker, E., 1990, "Use of satellite data to validate the hydrological cycle of the ECMWF model", *ECMWF/WCRP workshop, Cloud, radiative transfer and the hydrological cycle.* ECMWF Reading, UK., 179-197.

Le Marshall, J. F., 1988, "An intercomparison of temperature and moisture fields derived from TIROS Operational Vertical Sounder data by different retrieval techniques", *J. Appl. Meteor.*, 27 : 1282-1293.

Lipton, A. E., D. W. Hillger and T. H. Vonder Haar, 1986, "Water vapor vertical profile structures retrieved from satellite data via classification and determination", *Mon. Wea. Rev.*, 114 : 1103-1111.

McGuirk, J. P., L. L. Anderson and A. H. Thompson, 1985, "Satellite-derived synoptic climatology in data-sparse regions", *Adv. Space Res.*, 5167: 45-48.

-----, A. H. Thompson and N. R. Smith, 1987, "Moisture bursts over the tropical Pacific Ocean", *Mon. Wea. Rev.*, 115 : 787-798.

McMillin, L. M., and D. S. Crosby, 1984, "Theory and validation of the multiple window sea surface temperature technique" *J. Geophys. Res.*, 89 : 3655-3661.

Reuter, D., J. Susskind and A. Pursch, 1988, "First-guess dependence of a physically based set of temperature-humidity retrievals from HIRS2/MSU data", *J. Atmos. Oceanic Technol.*, 5 : 70-83.

Saito, K., and A. Baba, 1988, "A statistical relation between relative humidity and the GMS observed cloud amount", *J. Meteor. Soc. Japan*, 66 : 1987-1992.

Smith, D. E. W., 1989, "A comparison of model-generated and satellite-observed radiances", M.S. Thesis. Dept. of Meteorology, Texas A&M University, College Station, TX 77843, 150pp.

Smith, C. Hayden, D. Wark and L. M. McMillin, 1979, "The TIROS-N operational vertical sounder", *Bull. Amer. Meteor. Soc.*, 60 : 1177-1187.

-----, and H. M. Woolf, 1976, "The use of eigenvectors of statistical covariance matrices for interpreting satellite sounding radiometer observations", *J. Atmos. Sci.*, 33 : 1127-1140.

Staelin, D. H., K. F. Kunzi, R. L. Pettyjohn, R. K. L. Poon, R. W. Wilcox and J. W. Waters, 1976, "Remote sensing of atmospheric water vapor and liquid water with the Nimbus 5 microwave spectrometer", *J. Appl. Meteor.*, 15 : 1204-1214.

Tjemkes, S. A., and G. L. Stephens, 1990, "Intercomparison between microwave and infrared observations of precipitable water", *Fifth Conf on Satellite Meteorology and Oceanography*. London, England, Amer. Meteor. Soc., 82-86.

Wang, J. R., T. T. Wilheit and L. A. Chang, 1989, "Retrieval of total precipitable water using radiometric measurements near 92 and 183 GHz", *J. Appl. Meteor.*, 28 : 146-154.

Wilheit, T. T., 1990, "An algorithm for retrieving water vapor profiles in clear and cloudy atmospheres from 183 GHz radiometric measurements: Simulation studies", *J. Appl. Meteor.*, 29 : 508-515.